Quasiparticle properties of a simple metal at high electron temperatures

Lorin X. Benedict
H Division, Physics and Advanced Technologies Directorate, Lawrence Livermore National Laboratory, University of California, Livermore, California 94550

Catalin D. Spataru and Steven G. Louie
Department of Physics, University of California at Berkeley, Berkeley, California 94720
and Materials Sciences Division, Lawrence Berkeley National Laboratory, Berkeley, California 94720
(Received 26 June 2001; revised manuscript received 28 February 2002; published 29 August 2002)

We compute the real and imaginary parts of the quasiparticle self-energy Σ due to the electron-electron interaction for electrons and holes in jellium and crystalline Al at electron temperatures approaching the Fermi temperature T_F. $\mathrm{Re}\,\Sigma$ and $\mathrm{Im}\,\Sigma$ are computed using a finite temperature generalization of the GW approximation. We find a decrease in the electron lifetime and an increase in the valence and conduction bandwidths as T is increased. Calculation of the spectral function $A(k,E)$ reveals that the total weight in the quasiparticle peak is a very weak function of T, and that the basic peak structure remains for $T \sim \mathrm{few} \times 0.1 T_F$. These predictions suggest that at these electron temperatures, the prominent peak in the absorption spectrum of Al at ~ 1.5 eV should be washed out due to lifetime broadening, even if the ions remain in their crystalline positions.

DOI: 10.1103/PhysRevB.66.085116 PACS number(s): 71.10.Ca, 71.15.Qe

I. INTRODUCTION

Experimental and theoretical advances over the past few years have made it possible to investigate the properties of solid-density matter at extreme temperatures. On the experimental front, shock experiments,[1] and laser and resistive heating measurements[2] probe the equation of state and radiative properties of hot dense materials. On the theoretical side, high-temperature local-density approximation (LDA) calculations using the Mermin formulation have been applied to the Hugoniot equation of state of Al, exhibiting excellent agreement with the shock data.[3] In such a theoretical treatment, individual single-particle energies and wave functions appear only through the total electron density and the (suitably weighted) sum over occupied electron energies in the construction of the free energy. This is in the spirit of the density-functional prescription, appropriate for the determination of properties involving the thermodynamic ground state. In contrast, determination of spectroscopic properties (optical absorption, photoemission, etc.) typically involves explicit reference to single-particle-like excitations. Computations of the optical conductivity of hot dense Al have recently appeared which make use of the single-particle states of a high-temperature density-functional calculation.[4]

One of the most useful concepts in understanding condensed-matter spectroscopy is the notion of a quasiparticle.[5] This object, consisting of a particle together with its surrounding screening cloud, can be thought of as interacting only weakly with other quasiparticles, thereby justifying an effective independent particle picture. A familiar use of this concept is in the computation of the optical absorption spectrum within the random-phase approximation (RPA). Here, absorption of a photon by a many-electron system can be thought of as excitation of an individual quasielectron from one quasiparticle state to another. Such a description requires that the quasiparticle concept be meaningful, and in particular that the quasiparticle lifetimes are long. This is always a good assumption for a simple metal as long as the temperature is low, and the quasiparticle energy is close to the Fermi energy E_F.[5]

Unfortunately, the meaningfulness of the quasiparticle concept is not at all guaranteed when the electron temperature T is of the order of the Fermi temperature T_F. The large number of final states available at high T facilitates the rapid decay of a quasielectron via emission and absorption of plasmons and electron-hole pairs. In addition, even if the quasiparticle approximation is justified, we might still expect significant renormalizations of the quasiparticle energies due to the electron-electron interaction, since such self-energy corrections (to bandwidths and band gaps) computed in the GW approximation are already important at $T=0$.[6] It is not clear, *a priori*, as to what the T dependence of these corrections should be.

To this end, we present calculations of the real and imaginary parts of the electron self-energy operator Σ due to electron-electron interaction and determined with a finite-T variant of the GW approximation. We first consider electrons and holes in jellium, in an attempt to generalize early work on the electron gas[7] to high temperatures. For all calculations, we focus on densities comparable to that of solid Al ($r_s=2$), and T between 0 and T_F. By computing $\mathrm{Im}\,\Sigma(k, E=\hbar^2k^2/2m)$ and $\mathrm{Re}\,\Sigma(k, E=\hbar^2k^2/2m)$, we show that the inverse lifetime increases with T as expected,[5] as does the quasiparticle bandwidth. Calculation of the spectral function $A(k,E)$ demonstrates that (at least within the single-iteration GW approximation) the quasiparticle peak is broadened, but remains well defined and separated from the satellite peaks at the temperatures of interest. We then consider crystalline Al at high electron T, relevant for the understanding of subsequent ultrashort pulsed laser pump-probe measurements.[8] Here we compute $\mathrm{Im}\,\Sigma(\mathbf{k}, E=E_{\mathbf{k}})$ and $\mathrm{Re}\,\Sigma(\mathbf{k}, E=E_{\mathbf{k}})$ within the GW approximation, using *ab initio* pseudopoten-

tial LDA band energies and wave functions. We show that these results are remarkably similar to the jellium results for $r_s=2$, suggesting that details of the Fermi surface, etc. are not crucial to understanding the qualitative features of the energy-dependent quasiparticle lifetimes and energies of this system. We then argue that at these electron temperatures, the inclusion of quasiparticle lifetime effects should wash out a prominent feature in the absorption spectrum arising from transitions between parallel bands.

Section II contains the derivation of our finite-T GW expressions using the Matsubara Green's-function technique, and a discussion of the computational details for jellium and crystalline Al calculations. Sec. III presents the results along with a discussion of our findings. We conclude in Section IV.

II. THEORY AND COMPUTATION

A. Formalism for the calculation of Re Σ and Im Σ

We consider a spatially inhomogeneous many-electron system[9] at temperature T with an electron-electron interaction $v(\mathbf{r},\mathbf{r}')$. The homogeneous (jellium) system is considered later as a special case. The expression for the quasiparticle self-energy in the GW approximation is

$$\Sigma(\mathbf{r},\mathbf{r}';i\nu_n)=-\frac{1}{\beta}\sum_{i\omega_m} G(\mathbf{r},\mathbf{r}';i\nu_n-i\omega_m)W(\mathbf{r},\mathbf{r}';i\omega_m), \tag{1}$$

where G is the one-electron Green's function, W $(=\epsilon^{-1}v)$ is the screened interaction, ν_n and ω_m are Matsubara frequencies equal to $(2n+1)\pi/\beta$ and $2m\pi/\beta$, respectively, and $\beta=1/(k_BT)$. Writing G and W in their spectral representations, we have

$$G(\mathbf{r},\mathbf{r}';i\nu_n)=\frac{1}{\pi}\int_{-\infty}^{\infty}dE\frac{\mathrm{Im}\,G(\mathbf{r},\mathbf{r}';E)}{i\nu_n-E}, \tag{2}$$

$$W(\mathbf{r},\mathbf{r}';i\omega_m)=v(\mathbf{r},\mathbf{r}')+\frac{1}{\pi}\int_0^{\infty}dE\frac{2E\,\mathrm{Im}\,W(\mathbf{r},\mathbf{r}';E)}{\omega_m^2+E^2}. \tag{3}$$

If we plug these expressions into Eq. (1), evaluate the sums over $i\omega_m$,[10] and perform the Wick rotation $i\nu_n\to E+i\delta$, we obtain an expression for the retarded $\Sigma(E)$,

$$\begin{aligned}\Sigma(\mathbf{r},\mathbf{r}';E)=&-\frac{1}{\pi}\int_{-\infty}^{\infty}dE'\,\mathrm{Im}\,G(\mathbf{r},\mathbf{r}';E')n_F(E')v(\mathbf{r},\mathbf{r}')\\&-\frac{1}{\pi}\int_{-\infty}^{\infty}dE'\,\mathrm{Im}\,G(\mathbf{r},\mathbf{r}';E')\\&\times\frac{1}{\pi}\int_0^{\infty}dE''\mathrm{Im}\,W(\mathbf{r},\mathbf{r}';E'')\\&\times\left[\frac{n_F(E')-n_B(E'')-1}{E'-E+E''+i\delta}+\frac{n_F(E')+n_B(E'')}{E+E''-E'-i\delta}\right],\end{aligned} \tag{4}$$

where $n_F(E)=1/\{\exp[\beta(E-\mu)]+1\}$ and $n_B(E)=1/[\exp(\beta E)-1]$ are the usual statistical factors for a system of fermions (with T-dependent chemical potential μ) and a system of bosons, respectively. Finally, we replace $v(\mathbf{r},\mathbf{r}')$ in the above expression by $W(\mathbf{r},\mathbf{r}';E'-E)$ using Eq. (3) (with $i\omega_m\to E'-E+i\delta$), and collect terms to get[11]

$$\begin{aligned}\Sigma(\mathbf{r},\mathbf{r}';E)=&-\frac{1}{\pi}\int_{-\infty}^{\infty}dE'\,\mathrm{Im}\,G(\mathbf{r},\mathbf{r}';E')\\&\times W(\mathbf{r},\mathbf{r}';E'-E)n_F(E')\\&-\frac{1}{\pi}\int_{-\infty}^{\infty}dE'\,\mathrm{Im}\,G(\mathbf{r},\mathbf{r}';E')\\&\times\frac{1}{\pi}\int_0^{\infty}dE''\mathrm{Im}\,W(\mathbf{r},\mathbf{r}';E'')\\&\times\left[\frac{1+n_B(E'')}{E-E'-E''-i\delta}+\frac{n_B(E'')}{E-E'+E''-i\delta}\right].\end{aligned} \tag{5}$$

We evaluate the above expression in a first-order approximation by assuming that the spectral weight in G is entirely taken up in quasiparticle peaks. In other words, we take G to be the *noninteracting* Green's function, with

$$\begin{aligned}\mathrm{Im}\,G(\mathbf{r},\mathbf{r}';E)&=\pi A(\mathbf{r},\mathbf{r}';E)\\&=\pi\sum_{n,\mathbf{k}}\phi_{n,\mathbf{k}}(\mathbf{r})\phi^*_{n,\mathbf{k}}(\mathbf{r}')\,\delta(E-E_{n,\mathbf{k}}),\end{aligned} \tag{6}$$

where $\phi_{n,\mathbf{k}}(\mathbf{r})$ and $E_{n,\mathbf{k}}$ are wave functions and energies of single-particle states from, say, an LDA calculation for a crystalline system. Using Eqs. (5) and (6), together with the periodic translational invariance of the crystal, we can write down expressions for the matrix elements of the Σ operator between two Bloch states. The matrix element of Re Σ is[11]

$$\begin{aligned}&\langle n,\mathbf{k}|\mathrm{Re}\,\Sigma(\mathbf{r},\mathbf{r}';E)|n',\mathbf{k}\rangle\\&=-\sum_{n_1}\sum_{\mathbf{q},\mathbf{G},\mathbf{G}'}M^{\mathbf{G}}_{n,n_1}(\mathbf{k},\mathbf{q})[M^{\mathbf{G}'}_{n',n_1}(\mathbf{k},\mathbf{q})]^*v(\mathbf{q}+\mathbf{G}')\\&\times\frac{1}{\pi}\mathrm{P}\int_{-\infty}^{\infty}dE'\,\mathrm{Im}\,\epsilon^{-1}_{\mathbf{G},\mathbf{G}'}(\mathbf{q},E')\\&\times\left[\frac{1+n_B(E')}{E-E_{n_1,\mathbf{k}-\mathbf{q}}-E'}-n_F(E_{n_1,\mathbf{k}-\mathbf{q}})\right].\end{aligned} \tag{7}$$

The matrix element of Im Σ is

$$\langle n,\mathbf{k}|\mathrm{Im}\,\Sigma(\mathbf{r},\mathbf{r}';E)|n',\mathbf{k}\rangle$$

$$=\sum_{n_1}\sum_{\mathbf{q},\mathbf{G},\mathbf{G}'} M^{\mathbf{G}}_{n,n_1}(\mathbf{k},\mathbf{q})[M^{\mathbf{G}'}_{n',n_1}(\mathbf{k},\mathbf{q})]^* v(\mathbf{q}+\mathbf{G}') \times \mathrm{Im}\,\epsilon^{-1}_{\mathbf{G},\mathbf{G}'}(\mathbf{q},E-E_{n_1,\mathbf{k}-\mathbf{q}}) \times[1+n_B(E-E_{n_1,\mathbf{k}-\mathbf{q}})-n_F(E_{n_1,\mathbf{k}-\mathbf{q}})]. \quad (8)$$

In Eqs. (7) and (8), $\mathbf{q}$ is a wave vector in the first Brillouin zone (BZ), $\mathbf{G}$ and $\mathbf{G}'$ are reciprocal-lattice vectors, (n, n', n_1) are band indices, and $M^{\mathbf{G}}_{n,n_1}(\mathbf{k},\mathbf{q})=\langle n,\mathbf{k}|e^{i(\mathbf{q}+\mathbf{G})\cdot\mathbf{r}}|n_1,\mathbf{k}-\mathbf{q}\rangle$. The dielectric function appearing in the above expressions, ϵ, is related to the polarizability χ through the relation $\epsilon(\mathbf{r},\mathbf{r}';E)=\delta(\mathbf{r}-\mathbf{r}')-\int d\mathbf{r}'' v(\mathbf{r}'',\mathbf{r}')\chi(\mathbf{r},\mathbf{r}'';E)$. We compute the polarizability in the RPA,

$$\chi(\mathbf{r},\mathbf{r}';i\omega_m)=-\frac{1}{\beta}\sum_{i\nu_n} G(\mathbf{r},\mathbf{r}';i\omega_m-i\nu_n)G(\mathbf{r},\mathbf{r}';i\nu_n). \quad (9)$$

Fourier transformation, summation over $i\nu_n$, and analytic continuation to real energy yields the expression for ϵ at nonzero-T:

$$\epsilon_{\mathbf{G},\mathbf{G}'}(\mathbf{q},\omega)=\delta_{\mathbf{G},\mathbf{G}'}-\frac{4\pi e^2}{|\mathbf{q}+\mathbf{G}|^2}\sum_{n,n',\mathbf{k}} M^{\mathbf{G}}_{n,n'}(\mathbf{k},\mathbf{q}) \times[M^{\mathbf{G}'}_{n,n'}(\mathbf{k},\mathbf{q})]^*\frac{n_F(E_{n',\mathbf{k}-\mathbf{q}})-n_F(E_{n,\mathbf{k}})}{E_{n',\mathbf{k}-\mathbf{q}}-E_{n,\mathbf{k}}+\hbar\omega+i\delta}. \quad (10)$$

B. Computational details

Renormalized quasiparticle wave functions, energies, and lifetimes can be determined from Σ through the quasiparticle equation

$$\left[H_0+\Sigma\left(\mathbf{r},\mathbf{r}';E_{n,\mathbf{k}}-i\frac{\tau^{-1}_{n,\mathbf{k}}}{2}\right)\right]\psi_{n,\mathbf{k}}(\mathbf{r}) =\left(E_{n,\mathbf{k}}-i\frac{\tau^{-1}_{n,\mathbf{k}}}{2}\right)\psi_{n,\mathbf{k}}(\mathbf{r}),$$

where H_0 is the LDA (or other mean-field) Hamiltonian containing kinetic, electron-ion, and Hartree terms, but excluding the exchange-correlation term. In principle, this equation should be solved to self-consistency to obtain the quasiparticle wave functions, $\psi_{n,\mathbf{k}}$, quasiparticle energies $E_{n,\mathbf{k}}$, and quasiparticle lifetimes $\tau_{n,\mathbf{k}}$. We assume, as in previous work,[6] that the quasiparticle wave functions are close to the unrenormalized wave functions and compute quasiparticle energies by first-order perturbation in Σ,

$$E_{n,\mathbf{k}}=E^{LDA}_{n,\mathbf{k}}+Z_{n,\mathbf{k}}\langle n,\mathbf{k}|[\mathrm{Re}\,\Sigma(\mathbf{r},\mathbf{r}';E^{LDA}_{n,\mathbf{k}})-v_{xc}(\mathbf{r})]|n,\mathbf{k}\rangle. \quad (11)$$

$Z_{n,\mathbf{k}}=[1-\partial\mathrm{Re}\,\Sigma(\omega)/\partial\omega|_{E^{LDA}_{n,\mathbf{k}}}]^{-1}$ is the renormalization factor, $|n,\mathbf{k}\rangle$ is the unrenormalized (e.g. LDA) state, $E^{LDA}_{n,\mathbf{k}}$ is the unrenormalized energy, and $v_{xc}(\mathbf{r})$ is the mean-field exchange-correlation potential. We compute the quasiparticle lifetimes $\tau_{n,\mathbf{k}}$ from the equation[12]

$$\frac{1}{\tau_{n,\mathbf{k}}}=-2Z_{n,\mathbf{k}}\langle n,\mathbf{k}|\mathrm{Im}\,\Sigma(\mathbf{r},\mathbf{r}';E_{n,\mathbf{k}})|n,\mathbf{k}\rangle. \quad (12)$$

The matrix elements, $\langle n,\mathbf{k}|\mathrm{Re}\,\Sigma|n,\mathbf{k}\rangle$ and $\langle n,\mathbf{k}|\mathrm{Im}\,\Sigma|n,\mathbf{k}\rangle$, are calculated with Eqs. (7) and (8). For the jellium case, $v_{xc}(\mathbf{r})$ is a constant, so we do not include it in the determination of the band energies. It should be noted that the quantity $Z_{n,\mathbf{k}}$ is equal to the amount of spectral weight under the quasiparticle peak of the electron spectral function. This will be discussed further in the next section.

Because we are considering the many-electron system at high T, H_0 should be T dependent. Self-consistent calculations with T-dependent Hartree and electron-ion terms suggest that the unrenormalized energies and wave functions are only weakly dependent on T for crystalline Al at the temperatures of interest to us[13] (while for jellium, this is simply not an issue). Thus, we take H_0 to be the $T=0$ mean-field Hamiltonian, and include all T-dependent corrections through the self-energy.

We now describe some of the calculational details for our evaluation of Eqs. (7),(8), and, (10) for the cases of jellium and crystalline Al. In jellium, all two-point functions depend only on $|\mathbf{r}-\mathbf{r}'|$ rather than on $\mathbf{r}$ and $\mathbf{r}'$ separately. So the only nonzero elements in reciprocal space correspond to $\mathbf{G}=\mathbf{G}'=0$. Furthermore, the single-particle eigenstates arise from a single band and are of the form $\langle\mathbf{r}|\mathbf{k}\rangle=(1/\sqrt{\Omega})e^{i\mathbf{k}\cdot\mathbf{r}}$. This eliminates the sum over bands, and all nonzero matrix elements, $M^{\mathbf{G}}_{n,n_1}(\mathbf{k},\mathbf{q})$, are equal to unity. The expression for ϵ in Eq. (10) reverts to the nonzero-T Lindhard formula. Though this is easily evaluated directly for infinitesimal broadening, $\delta\to 0$ (the imaginary part ϵ_2 can be written down analytically in this case), the resulting poles in ϵ^{-1} are infinitesimally narrow if T is much less than T_F. This makes the sums over $\mathbf{q}$ in Eqs. (7) and (8) very difficult to evaluate when $\mathbf{q}$ is small. We choose to introduce a nonzero broadening which in turn enables us to perform this sum with a reasonable number of $\mathbf{q}$ points. This is acceptable as long as the final results are independent of the broadening chosen. We compute ϵ_2 from the expression

$$\epsilon_2(q,\omega)=\frac{\Omega}{2\pi}\int_0^\infty\frac{p^2dp}{e^{\beta(E_p-\mu)}+1}\int_{-1}^{1}d\gamma \times\left[L\left(E_q+\frac{\hbar pq\gamma}{m}-\hbar\omega;\delta\right) -L\left(E_q+\frac{\hbar pq\gamma}{m}+\hbar\omega;\delta\right)\right], \quad (13)$$

where $L(x;\delta)=(\delta/\pi)/(x^2+\delta^2)$ is a Lorentzian of width δ, $E_p=\hbar^2p^2/2m$, and $E_q=\hbar^2q^2/2m$. After this integral is per-

formed numerically, $\epsilon_1(q,\omega)$ is obtained by numerical Kramers-Kronig transform. Reϵ^{-1} and Im ϵ^{-1} are then computed from ϵ_1 and ϵ_2.

The expressions of Eqs. (7) and (8) are of the form $\langle \mathbf{k}|\Sigma(E)|\mathbf{k}\rangle = \int d^3q v(q) F(\mathbf{k},E,\mathbf{q})$. For an isotropic system like jellium, we are free to choose $\mathbf{k}=k\hat{\mathbf{z}}$. Then the integrands F can be shown to depend on $\mathbf{q}$ only through its magnitude, q, and $\mathbf{k}\cdot\mathbf{q}=kq\nu$. Thus we can write

$$\langle k|\Sigma(E)|k\rangle = 2\pi \int_0^\infty q^2 dq v(q) \int_{-1}^{1} d\nu F(k,E,\nu,q),$$

so we reduce the three-dimensional integral to two successive one-dimensional integrals. An added feature is that the q^2 factor in the volume element cancels the $1/q^2$ in $v(q)$, making it unnecessary for us to consider the long-wavelength limit separately, as is often done in *GW* calculations performed on a three-dimensional mesh of $\mathbf{q}$ points. The γ integration of Eq. (13) is performed analytically. For the p integral, we use 2000 points, and integrate up to a maximum p of $10k_F$. The inverse dielectric function is tabulated for 2000 q points (from 0 to $10k_F$) and 400 ω points (from 0 to $4E_F$). In the determination of the self-energy matrix elements, we use 200 ν integration points, and 2000 q points, and integrate up to a $q_{\max}$ of $10k_F$. The expression for $\langle k|\mathrm{Re}\,\Sigma|k\rangle$ involves an integral over energy [E' in Eq. (7)]. We use 400 integration points and take the upper limit of integration to be $4E_F$. There are two positive infinitesimals used in the calculation. We use 0.2 eV for the Lorentzian broadening in Eq. (13), and a very small broadening of 0.005 eV is used to take the principal part of the integrals involved in the Kramers-Kronig transform of ϵ_2, as well as the principal part of the integral in Eq. (7). These choices produce converged results for the densities ($r_s \sim 2$) and temperatures (T between 0 and T_F) of interest to us.

For crystalline Al, we use Eqs. (7), (8), and (10) exactly as written, and take single-particle wave functions $\phi_{n,\mathbf{k}}(\mathbf{r})$ and energies $E_{n,\mathbf{k}}$ from *ab initio* pseudopotential LDA calculations performed at the experimental lattice constant. The cutoff in $\mathbf{G}$ space with which the wave functions are expanded is taken to be 6 Ry. We use 60 valence plus conduction bands and discrete meshes of $\mathbf{q}$ points ($6\times6\times6$ and $8\times8\times8$) in the first BZ in the sums of Eqs. (7), (8), and (10).[14] We use 333 E' points and an upper limit of 100 eV in the integration of Eq. (7). The broadening in Eq. (10) is chosen to be 0.3 eV, consistent with the size of our $\mathbf{k}$ point mesh, and adequate for evaluating the sums over $\mathbf{q}$ in Eqs. (7) and (8). As mentioned above, our use of a discrete mesh in $\mathbf{q}$ space forces us to treat the $\mathbf{q}\to0$ case separately, as discussed by Hybertsen and Louie[6] for $T=0$. The $T>0$ case we consider here poses no extra difficulties in this regard. Finally, we find it necessary to eliminate the divergence in $n_B(E)$ as $E\to0$ in order to obtain converged results at high T for both Al and jellium calculations. We handle this by setting $n_B=n_{Bmax}$ if $n_B>n_{Bmax}$. As long as n_{Bmax} is chosen to be between 10^2 and 10^5, our results are independent of the precise choice.

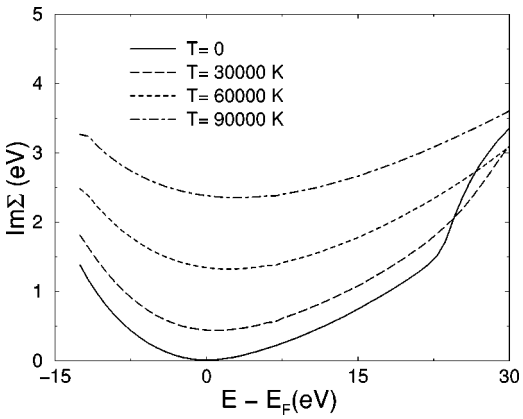

FIG. 1. $|\mathrm{Im}\,\Sigma(k,E=\hbar^2k^2/2m)|$ vs $E-E_F$ for jellium at a density given by $r_s=2.0$ and $T=0$, $0.2E_F$, $0.4E_F$, and $0.6E_F$, where $E_F=12.5$ eV ($\sim$150 000 K) is the Fermi energy at $T=0$.

III. RESULTS AND DISCUSSION

A. Jellium

We estimate the temperature dependence of the quasiparticle lifetimes by computing $\mathrm{Im}\,\Sigma(k,E=\hbar^2k^2/2m)$ from the procedures outlined above. Figure 1 shows $|\mathrm{Im}\,\Sigma|$ as a function of $E-E_F$ for the $r_s=2.0$ electron gas at $T=0$, $0.2E_F$, $0.4E_F$, and $0.6E_F$, where $E_F=$ 12.5 eV is the Fermi energy at $T=0$. Our $T=0$ result is essentially identical to that of B.I. Lunqvist.[7] In particular, at the Fermi energy, $\mathrm{Im}\,\Sigma=0$ (so the lifetime is infinite at $T=0$), and $|\mathrm{Im}\,\Sigma|$ increases quadratically away from E_F. At nonzero T, there is no energy for which the quasielectron lifetime is infinite, and the minimum value of $|\mathrm{Im}\,\Sigma|$ increases with T. Note, however, that the approximate quadratic behavior away from the minimum is retained.

The temperature dependence seen in Fig. 1 can be understood by examining Eqs. (8) and (10). Here, the temperature dependence is contained entirely in the statistical factors, $n_F(E)$ and $n_B(E)$. The $T\to0$ limit corresponds to taking $n_F(E)\to\theta(\mu-E)$ and $n_B(E)\to\theta(E)-1$. Although Eq. (8) presents a compact way of writing $\mathrm{Im}\,\Sigma$, a more physically intuitive expression can be obtained by decomposing the right-hand side into four terms, representing four distinct decay processes (we supress matrix elements, $\mathbf{G}$ vectors, and band indices for simplicity): electron with emission, hole with emission, electron with absorption, and hole wih absorption,

$$\langle \mathbf{k}|\mathrm{Im}\,\Sigma|\mathbf{k}\rangle = \langle \mathbf{k}|\mathrm{Im}\,\Sigma_{ee}|\mathbf{k}\rangle + \langle \mathbf{k}|\mathrm{Im}\,\Sigma_{he}|\mathbf{k}\rangle + \langle \mathbf{k}|\mathrm{Im}\,\Sigma_{ea}|\mathbf{k}\rangle + \langle \mathbf{k}|\mathrm{Im}\,\Sigma_{ha}|\mathbf{k}\rangle.$$

$$\langle \mathbf{k}|\mathrm{Im}\,\Sigma_{ee}|\mathbf{k}\rangle = \sum_{\mathbf{q}} \mathrm{Im}\,\epsilon^{-1}(\mathbf{q},E-E_{\mathbf{k}-\mathbf{q}}) v(\mathbf{q}) \times [1+n_B(E-E_{\mathbf{k}-\mathbf{q}})][1-n_F(E_{\mathbf{k}-\mathbf{q}})]\theta(E-E_{\mathbf{k}-\mathbf{q}}),$$

$$\langle \mathbf{k}|\mathrm{Im}\,\Sigma_{\mathrm{he}}|\mathbf{k}\rangle = \sum_{\mathbf{q}} \mathrm{Im}\,\epsilon^{-1}(\mathbf{q}, E_{\mathbf{k}-\mathbf{q}} - E) v(\mathbf{q}) \times [1 + n_B(E_{\mathbf{k}-\mathbf{q}} - E)] n_F(E_{\mathbf{k}-\mathbf{q}})\, \theta(E_{\mathbf{k}-\mathbf{q}} - E),$$

$$\langle \mathbf{k}|\mathrm{Im}\,\Sigma_{\mathrm{ea}}|\mathbf{k}\rangle = \sum_{\mathbf{q}} \mathrm{Im}\,\epsilon^{-1}(\mathbf{q}, E_{\mathbf{k}-\mathbf{q}} - E) \times v(\mathbf{q}) n_B(E_{\mathbf{k}-\mathbf{q}} - E)[1 - n_F(E_{\mathbf{k}-\mathbf{q}})] \times \theta(E_{\mathbf{k}-\mathbf{q}} - E),$$

$$\langle \mathbf{k}|\mathrm{Im}\,\Sigma_{\mathrm{ha}}|\mathbf{k}\rangle = \sum_{\mathbf{q}} \mathrm{Im}\,\epsilon^{-1}(\mathbf{q}, E - E_{\mathbf{k}-\mathbf{q}}) \times v(\mathbf{q}) n_B(E - E_{\mathbf{k}-\mathbf{q}}) n_F(E_{\mathbf{k}-\mathbf{q}})\, \theta(E - E_{\mathbf{k}-\mathbf{q}}).$$

Each term can be thought of as the transition rate for an electron or hole in state $|\mathbf{k}\rangle$ (with energy E) to decay into state $|\mathbf{k}-\mathbf{q}\rangle$ by emitting or absorbing a plasmon or electron-hole pair. $\mathrm{Im}\,\Sigma_{\mathrm{ee}}$ and $\mathrm{Im}\,\Sigma_{\mathrm{he}}$ are the only nonzero terms at $T=0$, due to the fact that the absorption terms are both proportional to numbers of plasmons excited prior to decay, which are zero at $T=0$. Note that the electron terms ($\mathrm{Im}\,\Sigma_{\mathrm{ee}}$ and $\mathrm{Im}\,\Sigma_{\mathrm{ea}}$) involve an electron in the state $|\mathbf{k}\rangle$ filling a hole in state $|\mathbf{k}-\mathbf{q}\rangle$, while the hole terms involve an electron in the state $|\mathbf{k}-\mathbf{q}\rangle$ filling a hole in state $|\mathbf{k}\rangle$. Each process contributes to the lifetime of $|\mathbf{k}\rangle$. Note also that $\mathrm{Im}\,\Sigma_{\mathrm{ee}}$ and $\mathrm{Im}\,\Sigma_{\mathrm{ha}}$ involve transitions in which $E > E_{\mathbf{k}-\mathbf{q}}$ while $\mathrm{Im}\,\Sigma_{\mathrm{he}}$ and $\mathrm{Im}\,\Sigma_{\mathrm{ea}}$ involve transitions with $E < E_{\mathbf{k}-\mathbf{q}}$.

Figure 2(a) shows the two nonzero (emission) terms as a function of energy for $T=0$ ($r_s=2.0$). $\mathrm{Im}\,\Sigma_{\mathrm{ee}}$ is nonzero only for $E > E_{\mathrm{F}}$, while $\mathrm{Im}\,\Sigma_{\mathrm{he}}$ is nonzero only for $E < E_{\mathrm{F}}$, due to the zero-temperature form of $n_F(E_{\mathbf{k}-\mathbf{q}})$. Figure 2(b) shows all four nonzero terms for $T=0.6E_{\mathrm{F}}$, along with their sum (which also appears in Fig. 1 as the 90 000-K data). The two emission terms are now nonzero at all energies, though $\mathrm{Im}\,\Sigma_{\mathrm{he}}$ is exponentially decreasing at high energies. This is because a nonzero $\mathrm{Im}\,\Sigma_{\mathrm{he}}$ requires that the state $|\mathbf{k}-\mathbf{q}\rangle$ be occupied, and the energies $E_{\mathbf{k}-\mathbf{q}}$ which contribute (roughly a plasmon energy above E) are quite high if E is above the Fermi energy. The electron with absorption term is appreciable at this temperature, and is roughly constant in energy, due to the requirement that the state $|\mathbf{k}-\mathbf{q}\rangle$ (with $E_{\mathbf{k}-\mathbf{q}} > E$) be empty, a condition easily met for all energies, as long as $\hbar\omega_p > E_{\mathrm{F}}$, as is the case for $r_s=2.0$. The hole with absorption term, on the other hand, decreases at high energies, because a nonzero $\mathrm{Im}\,\Sigma_{\mathrm{ha}}$ requires that the state $|\mathbf{k}-\mathbf{q}\rangle$ be occupied. Note that both absorption terms are, in general, smaller than the emission terms. The relatively small number of plasmons present at this temperature ensures this. As T increases, both absorption terms become more important, and eventually become comparable to the emission terms.

So we see that the temperature dependence of $|\mathrm{Im}\,\Sigma|$ in Fig. 1 is due to: (i) an increase in the plasmon population as T increases, which causes plasmon absorption and emission rates to increase, and (ii) increased availability of states into which electrons and holes can decay, which affects both

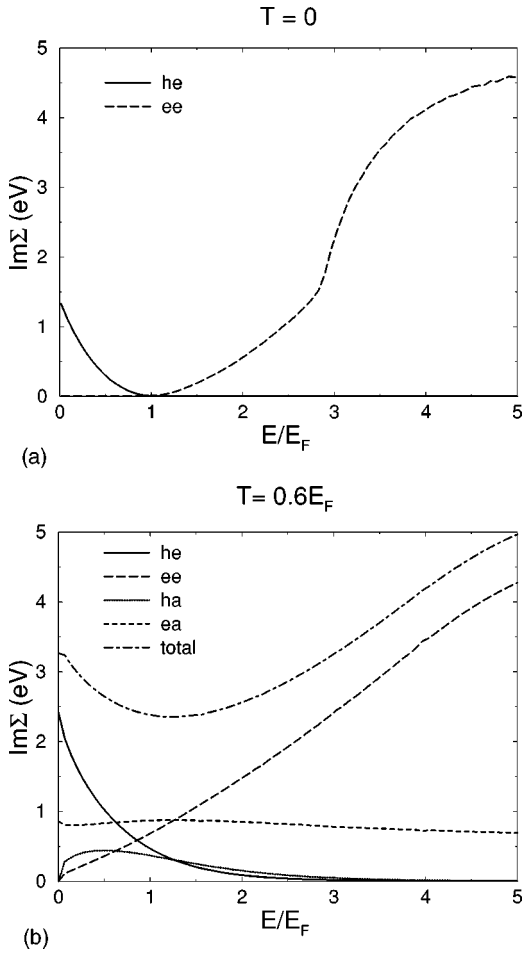

FIG. 2. Various terms (see text) contributing to $\mathrm{Im}\,\Sigma(k, E = \hbar^2k^2/2m)$ vs E/E_{F} for jellium with $r_s = 2.0$ at (a) $T=0$, and (b) $T=0.6E_{\mathrm{F}} \sim 90\,000$ K.

emission and absorption processes. In addition, there is the temperature dependence of the loss function, $\mathrm{Im}\,\epsilon^{-1}(\mathbf{q},\omega)$. Through the n_F factors in Eq. (10), the plasmon peaks at $\omega(\mathbf{q}\to 0) \sim \pm\sqrt{4\pi n e^2/m}$ are broadened at high T. This tends to smooth out the sharp features in the energy dependence of $\mathrm{Im}\,\Sigma$ seen at $T=0$ (see, for example, the disappearance of the kink at $E \sim 3E_{\mathrm{F}}$ for $T>0$ in Fig. 2). However, this effect is of secondary importance; if the zero-temperature $\mathrm{Im}\,\epsilon^{-1}(\mathbf{q},\omega)$ is used in the calculations of Figs. 1 and 2, the qualitative features remain the same.

In order to estimate temperature-dependent corrections to the noninteracting single-particle energies of a homogeneous electron gas, we compute $\mathrm{Re}\,\Sigma(k, E = \hbar^2k^2/2m)$. Figure 3 shows $\mathrm{Re}\,\Sigma$ as a function of $E - E_{\mathrm{F}}$ for an electron gas with $r_s = 2.0$ at temperatures of 0, $0.2E_{\mathrm{F}}$, $0.4E_{\mathrm{F}}$, and $0.6E_{\mathrm{F}}$. Again, our $T=0$ result is identical to that obtained by Lundqvist for $r_s = 2.0$.[7] Note that for $T=0$, $\mathrm{Re}\,\Sigma(E - E_{\mathrm{F}} < 15$ eV) is roughly constant. This means that if we use Eq. (11) to predict the quasiparticle energies ($Z_{k_{\mathrm{F}}}$ is also roughly constant for these energies, see below), the bottom of the band is shifted down by the same amount as the states at E_{F}. The occupied bandwidth is therefore relatively unchanged. As T is increased, $\mathrm{Re}\,\Sigma$ increases with energy; states at the

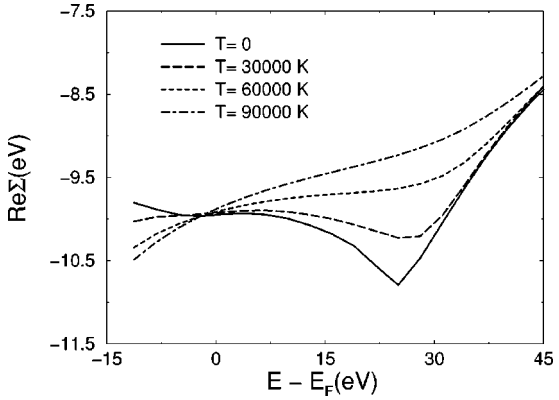

FIG. 3. $\mathrm{Re}\,\Sigma(k,E=\hbar^2k^2/2m)$ vs $E-E_\mathrm{F}$ for jellium at a density given by $r_s=2.0$ and $T=0$, $0.2E_\mathrm{F}$, $0.4E_\mathrm{F}$, and $0.6E_\mathrm{F}$, where $E_\mathrm{F}=12.5$ eV ($\sim 150\,000$ K) is the Fermi energy at $T=0$.

bottom of the band are shifted down more than the higher energy states, so the bandwidth is widened. This widening is, however, quite small relative to the total bandwidth. For instance, for $T=0.6E_\mathrm{F}$, the band is widened by about 1.5 eV over a 50-eV range. Note that the dip at $E\sim 24$ eV disappears as T increases. It should be mentioned that we find the renormalization factor Z_{k_F} to be practically independent of T for this density (and for comparable densities). For $r_s=2.0$, our $T=0$ value is 0.77, in agreement with Lundqvist.[7] Though we find Z_{k_F} to increase monotonically with T, we compute it to be only 0.82 for $T=E_\mathrm{F}$.

All of the T-dependent changes to $\mathrm{Re}\,\Sigma$ can be interpreted as changes in the quasielectron effective mass due to the virtual emission and absorption of plasmons and electron-hole pairs at high T. In fact, there are four distinct virtual processes which are the exact analog of the four decay processes involved in $\mathrm{Im}\,\Sigma$. For example, one process involves an electron in state $|\mathbf{k}\rangle$ undergoing a virtual transition to the intermediate state $|\mathbf{k}-\mathbf{q}\rangle$, and then jumping back to $|\mathbf{k}\rangle$. If $E_{\mathbf{k}-\mathbf{q}}<E$, this second-order process, which renormalizes the energy of $|\mathbf{k}\rangle$, is the counterpart of what we called "electron with emission" above. The final state of the $\mathrm{Im}\,\Sigma$ process has become the intermediate state of a corresponding $\mathrm{Re}\,\Sigma$ process. Thus the decomposition $\langle\mathbf{k}|\mathrm{Re}\,\Sigma|\mathbf{k}\rangle=\langle\mathbf{k}|\mathrm{Re}\,\Sigma_{\mathrm{ee}}|\mathbf{k}\rangle+\langle\mathbf{k}|\mathrm{Re}\,\Sigma_{\mathrm{he}}|\mathbf{k}\rangle+\langle\mathbf{k}|\mathrm{Re}\,\Sigma_{\mathrm{ea}}|\mathbf{k}\rangle+\langle\mathbf{k}|\mathrm{Re}\,\Sigma_{\mathrm{ha}}|\mathbf{k}\rangle$ is possible. While we do not write expressions for each term here, they have been discussed elsewhere in the context of electrons renormalized by phonons.[15] The effect of these processes on $\mathrm{Re}\,\Sigma$ can best be understood by noting that $\mathrm{Re}\,\Sigma(E)$ and $\mathrm{Im}\,\Sigma(E)$ satisfy the Kramers-Kronig relation. Thus peaks or shoulders in one correspond to inflection points in the other. To wit, the dip in $\mathrm{Re}\,\Sigma$ at $E\sim 24$ eV for $T=0$ (see Fig. 3) can be thought of as arising from the shoulder at that energy in $\mathrm{Im}\,\Sigma$ (Ref. 7) (see the kink visible in Fig. 2(a) at $E/E_\mathrm{F}\sim 2.9$). This shoulder comes from strong plasmon emission which occurs if E is slightly larger than $\hbar\omega_p$. As T is increased, the shoulder broadens due to (i) increased importance of other proceses such as absorption, and (ii) broadening of the plasmon peak in $\mathrm{Im}\,\epsilon^{-1}(\mathbf{q},\omega)$. These same effects therefore cause the disappearence of the dip in $\mathrm{Re}\,\Sigma$.

In order to investigate the extent to which the interacting Green's function differs from the noninteracting one given in Eq. (6), we compute the electron spectral function, defined by $\mathrm{Im}\,G(\mathbf{r},\mathbf{r}';E)=\pi A(\mathbf{r},\mathbf{r}';E)$. It can be calculated from $\mathrm{Re}\,\Sigma$ and $\mathrm{Im}\,\Sigma$. In the $\mathbf{k}$ representation,

$$A(\mathbf{k},E)=\frac{1}{\pi}\frac{|\mathrm{Im}\,\Sigma(\mathbf{k},E+\mu)|}{[E+\mu-E^0_{\mathbf{k}}-\mathrm{Re}\,\Sigma(\mathbf{k},E+\mu)]^2-[\mathrm{Im}\,\Sigma(\mathbf{k},E+\mu)]^2}, \tag{14}$$

where μ is the T-dependent chemical potential. Note that this expression involves the self-energy *off the energy shell*, or $E\neq E_{\mathbf{k}}$. Figure 4(a) shows our results for $A(k,E)$ at $T=0$ for an electron gas with $r_s=2.0$.[7] The quasiparticle peak is infinitesimally narrow for $k=k_\mathrm{F}$, as it should be (the slight broadening is due to the small δ in our calculation of ϵ^{-1}). The satellite structure at roughly a plasmon energy away on either side of the quasiparticle peak corresponds to the coupled electron-plasmon excitations known as "plasmarons."[7] Figure 4(b) shows $A(k,E)$ for $T=0.4E_\mathrm{F}$. The quasiparticle peaks are significantly broadened, but the basic peak structure remains for each k. Even at $T=E_\mathrm{F}$ [Fig. 4(c)], we find that the remnants of quasiparticle and plasmaron features are clearly present. It is true, however, that spectral features for a given k move to higher E as T is increased, a result of the fact that μ decreases with T. It is interesting to note that the (approximate) total weight in the quasiparticle peak at $k=k_\mathrm{F}$ is roughly independent of T, a consequence of our observation above that Z_{k_F} is roughly independent of T. So although the quasiparticle peak is broadened at high T (resulting in a short lifetime), the quasiparticle is still a well-defined excitation in this theory, in the sense that it is distinct from the background and its total spectral weight is roughly constant. We find the near independence of Z_{k_F} on T for somewhat lower densities as well (e.g., $r_s=5.0$), where electron correlations are more important and Z_{k_F} is farther from unity.

B. Crystalline Al

A real material, such as Al, at a single temperature T describes a state in which the ions are in motion. At the T of interest to us in this work (i.e., far above melting), the ions would be in a fluid state. However, there is a class of experiments in which the system is best described by $T_{\mathrm{electron}}=T$

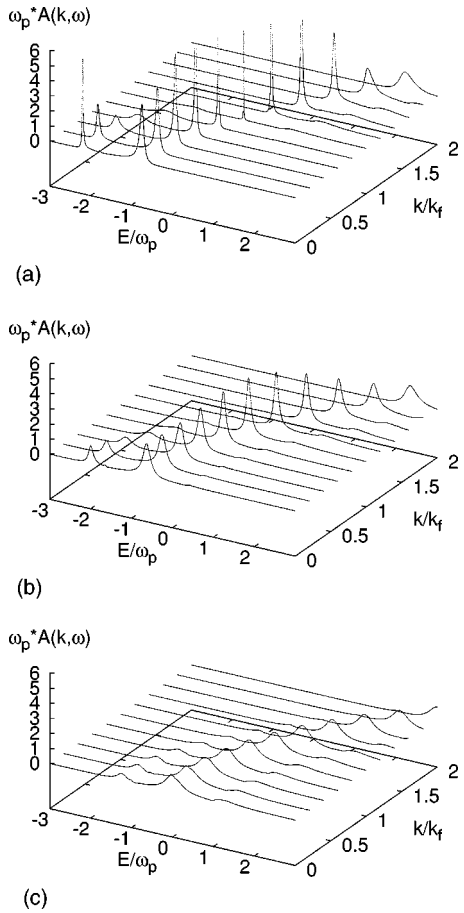

FIG. 4. $A(k,E)$ for k between 0 and $2k_F$ at (a) $T=0$, (b) $T=0.4E_F$, and (c) $T=E_F$, for jellium with $r_s=2.0$. In this figure, ω_p denotes the plasmon energy, $\hbar\sqrt{4\pi ne^2/m}$.

and $T_{ion}=0$. These are measurements performed with ultrashort pulsed lasers, in which the electrons are excited initially, and then (roughly a ps later) they exchange energy with the much heavier ions.[8] We perform *ab initio* calculations of the quasiparticle properties of crystalline Al at nonzero electron T in order to investigate the properties of the laser-excited metal *prior* to the motion of the ions.

Figure 5 shows $|\mathrm{Im}\,\Sigma(\mathbf{k},E=E_{\mathbf{k}}^{\mathrm{LDA}})|$ vs $E^{\mathrm{LDA}}-E_F$ for crystalline Al at electron temperatures of 0, 30 000, 60 000, and 90 000 K (which correspond to $T=0$, $0.23E_F$, $0.46E_F$, and $0.69E_F$, where E_F is the Fermi energy at $T=0$). With the exception of the noise in the curves, which is due primarilly to the use of a small discrete **k**-point mesh (but also to the dependence of Σ on the direction of **k**), the results are very similar to the $r_s=2.0$ jellium results at the corresponding temperatures. See, for example, the selected points from the jellium calculations appearing in Fig. 5. Thus the same quasiparticle lifetime found in jellium as T is increased is also seen for crystalline Al. Figure 6 shows $\mathrm{Re}\,\Sigma(\mathbf{k},E=E_{\mathbf{k}}^{\mathrm{LDA}})$ vs $E^{\mathrm{LDA}}-E_F$ for the same set of temperatures. Again the results are quite similar to those of jellium,[16] as seen by comparison with Fig. 3 (we refrain from including points from the jellium calculation in this figure, because absolute energies are different, and the scatter in the points from each curve is comparable to the spacing between

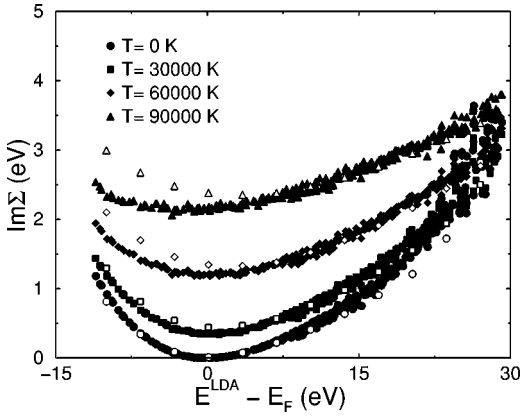

FIG. 5. $|\mathrm{Im}\,\Sigma(\mathbf{k},E=E_{\mathbf{k}}^{\mathrm{LDA}})|$ vs $E^{\mathrm{LDA}}-E_F$ for crystalline Al at electron T of 0, 30 000, 60 000, and 90 000 K. Open symbols represent selected data from the jellium results at the corresponding temperatures appearing in Fig. 1.

curves. The similarity with Fig. 3 is, however, readily apparent).[17] The deviation of the Al electronic structure from the free-electron picture (anisotropy of constant-energy surfaces in **k** space, avoided band crossings, complex spatial dependence of the periodic part of Bloch wave functions, etc.) does not seem to play a strong role in determining the T-dependent bandwidth and lifetime in crystalline Al.

Our calculations predict that crystalline Al at $T\sim$few $\times 0.1T_F$ will have the following features: (i) a quasiparticle bandwidth which increases with T, but only by a few percent; (ii) a quasiparticle inverse lifetime which increases rapidly with T, equal to several eV for $T\sim 10$ eV. What might be the experimental consequences of these predictions? A typical pump-probe experiment measures the optical conductivity $\sigma(\omega)$, or alternatively the imaginary part of the dielectric function $\epsilon_2(\omega)$. One way to calculate $\epsilon_2(\omega)$ would be to use Eq. (9), but with the *renormalized G* obtained from our self-energy calculations. Unfortunately, this suffers from the problem of neglecting vertex corrections,[18] a very serious problem when computing the response using renormalized propagators. A full, conserving calculation of the response including vertex corrections is extremely difficult and, to the best of our knowledge, has not yet been performed for an electron gas at $T=0$.[19] Thus it is beyond the scope of this

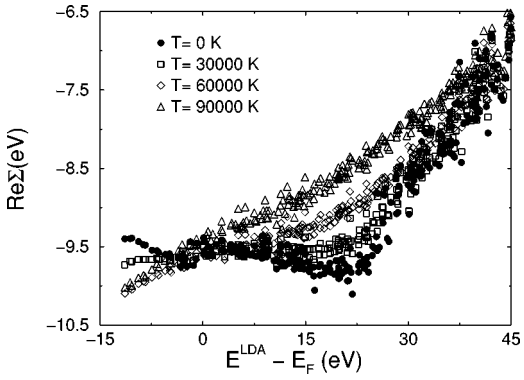

FIG. 6. $\mathrm{Re}\,\Sigma(\mathbf{k},E=E_{\mathbf{k}}^{\mathrm{LDA}})$ vs $E^{\mathrm{LDA}}-E_F$ for crystalline Al at electron T of 0, 30 000, 60 000, and 90 000 K.

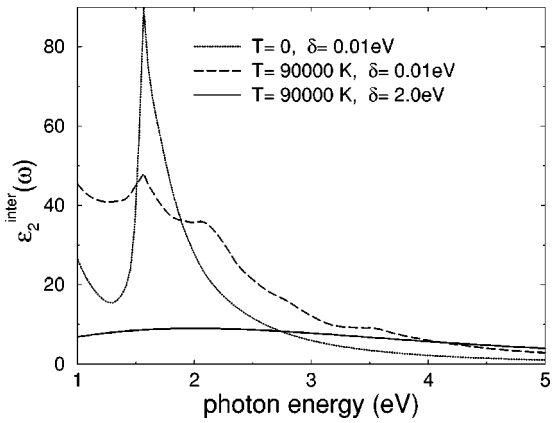

FIG. 7. $\epsilon_2^{inter}(\omega)$ for crystalline Al at $T=0$, and $T=90\,000$ K. The 90 000-K results are presented with two energy broadenings: 0.01 eV (meant to approximate the zero-broadening case), and 2.0 eV (consistent with our prediction of $|\mathrm{Im}\,\Sigma|$ for $T=90\,000$ K).

work. However, we can approximate the effects of this renormalization on $\epsilon_2(\omega)$ by performing an RPA [Eq. (10)] calculation for Al including the shift in the single-particle energies, and an energy broadening [given by δ in Eq. (10)] equal to the characteristic inverse lifetime. This is equivalent to the assumption that quasiparticle states before and after a scattering event are completely uncorrelated.[20] While this is incorrect in principle, the results should provide a reasonable qualitative picture of the response.

Figure 7 shows the results of our LDA calculations of $\epsilon_2^{inter}(\omega)$, the interband contribution to $\epsilon_2(\omega)$, for crystalline Al. The *intraband* contribution which we do not compute, $\epsilon_2^{intra}(\omega)$, is a smooth function peaked at $\omega=0$, devoid of structure (peaks) at high frequency. The dashed line represents the result for (electron temperature) $T=90\,000$ K, while the dotted line is the $T=0$ result. Both were computed with $\delta=0.01$ eV, consistent with the procedure for calculating the dielectric function at $T=0$ with a $32\times32\times32$ mesh of $\mathbf{k}$ points.[21] Note that although the 90 000-K spectrum is considerably broader, both curves exhibit a sharp peak at 1.55 eV resulting from transitions between a set of nearly parallel Al bands.[22] The solid line is the result of the same calculation, but with $\delta=2.0$ eV (consistent with the lifetime results at 90 000 K of Fig. 5). Renormalizing the band energies according to Fig. 6 produces negligible changes on this scale. Note that the magnitude of $\epsilon_2^{inter}(\omega)$ is significantly altered; spectral weight is spread out considerably, a consequence of the lifetime broadening. Note in particular that the prominent peak at $\hbar\omega\sim 1.55$ eV in the $T=0$ case (and present even in the $T=90\,000$-K case *without* lifetime broadening) is absent in the solid curve. This spectral feature is completely washed out once lifetime effects are included. Though the inclusion of vertex corrections may change this picture somewhat, we suggest that most or all of the spectral features arising from details in the band structure will be absent in the results of pump-probe experiments reaching such temperatures, *even during the short time that the material remains crystalline*.

Spectroscopy performed on liquid Al at high temperatures and near-solid densities is also of interest. The near equality of jellium and crystalline Al quasiparticle lifetimes presented here suggests that the jellium results should be relevant for liquid Al as well. Measurements and calculations on liquid Al at temperatures lower than those we consider here have already been reported.[2,4] RPA calculations of $\sigma(\omega)$ peformed by Silvestrelli show that ion disorder and thermal broadening of electron populations result in an effective Drude mean scattering time of $\sim\mathrm{few}\times10^{-16}$ s, leading to an energy broadening of $\sim1-10$ eV for Al at near-solid density and T between 1000 and 8000 K. This is comparable to the values that we compute due to electron-electron scattering at much higher T. While Silvestrelli's calculations using an infinitessimal lifetime broadening should be appropriate for the lower temperatures he considers, our results indicate that quasiparticle lifetime effects should contribute a significant component to the broadening of $\sigma(\omega)$ when $T\sim$ few $\times0.1T_\mathrm{F}$. However, since the ion disorder already contributes a significant broadening to the absorption spectrum in a liquid, the effect of quasiparticle lifetime broadening will be less pronounced than in the crystalline case.

IV. CONCLUSIONS

We have presented calculations of the real and imaginary parts of the electron self-energy operator for jellium ($r_s=2.0$) and crystalline Al (normal solid density) at high electron temperatures. The self-energy was computed with a nonzero-T variant of the GW approximation. We found bandwidths to increase and lifetimes to decrease with increasing temperature. Crystalline Al results were shown to be remarkably similar to those of jellium at the same density. In addition, we computed the spectral function for jellium and showed that quasiparticle and satellite peaks remain distinct at $T\sim\mathrm{few}\times0.1T_\mathrm{F}$, even though the quasiparticle peak is substantially broadened. We predict that optical conductivity experiments performed on solid-density Al reaching electron temperatures in excess of a few eV will not exhibit sharp features resulting from the band structure, even when the material is crystalline. Changes to the optical properties resulting from the renormalization of the bandwidth should not be apparent.

ACKNOWLEDGMENTS

We thank T. W. Barbee, III, M. P. Surh, E. L. Shirley, and D. Hess for helpful discussions. Collaborations between LLNL and LBNL were facilitated by the U.S. Department of Energy's Computational Materials Science Network. Portions of this work were performed under the auspices of the U.S. Department of Energy by University of California Lawrence Livermore National Laboratory under contract No. W-7405-Eng-48. This work was supported by the NSF under Grant No. DMR0087088, Office of Energy Research, Office of Basic Energy Sciences, Materials Sciences Division of the U.S. Department of Energy under Contract No. DE-AC03-76SF00098. Computer time was provided by the DOE at the Lawrence Berkeley National Laboratory's NERSC center.

[1] For a review of the technique, see L.V. Al'tshuler *et al.*, JAMTP **22**, 145 (1980).

[2] A.N. Mostovych and Y. Chan, Phys. Rev. Lett. **79**, 5094 (1997); J.F. Benage, W.R. Shanahan, and M.S. Murillo, *ibid.* **83**, 2953 (1999).

[3] M.P. Surh, T.W. Barbee, III, and L.H. Yang, Phys. Rev. Lett. **86**, 5958 (2001).

[4] P.L. Silvestrelli, Phys. Rev. B **60**, 16382 (1999).

[5] D. Pines and P. Nozieres, *The Theory of Quantum Liquids* (Addison-Wesley, Redwood City, CA, 1989), Vol. 1.

[6] L. Hedin and S. Lundqvist, Solid State Phys. **23**, 1 (1969); M.S. Hybertsen and S.G. Louie, Phys. Rev. B **34**, 5390 (1986); R.W. Godby, M. Schluter, and L.J. Sham, *ibid.* **37**, 10159 (1988).

[7] B.I. Lundqvist, Phys. Kondens. Mater. **6**, 193 (1967); **6**, 206 (1967); **7**, 117 (1968); Phys. Status Solidi **32**, 273 (1969).

[8] A. Forsman, A. Ng, G. Chiu, and R.M. More, Phys. Rev. E **58**, R1248 (1998).

[9] We consider systems with inversion symmetry in this work. For systems without inversion symmetry, the matrix elements, $M^{\mathbf{G}}_{n,n_1}(\mathbf{k},\mathbf{q})$ (appearing later), are complex. This affects the form of our expressions for the self-energy.

[10] G.D. Mahan, *Many Particle Physics* (Plenum, New York, 1981), pp. 157–159.

[11] Expressions for $\mathrm{Re}\,\Sigma$ and $\mathrm{Im}\,\Sigma$ at nonzero T for a homogeneous electron gas which are equivalent to ours appear in W. Fennel, W.D. Kraeft, and D. Kremp, Ann. Phys. (Leipzig) **7.**, Folge, Band 31, Heft 2 (1974), S.171-181.

[12] J.S. Dolgado, V.M. Silkin, M.A. Cazalilla, A. Rubio, and P.M. Echenique, Phys. Rev. B **64**, 195128 (2001).

[13] L.X. Benedict, M.P. Surh, and T.W. Barbee, III (unpublished).

[14] We used a $6\times6\times6$ mesh of $\mathbf{q}$ points for the determination of $\mathrm{Re}\,\Sigma$ because the integral over E' makes the calculation very computationally intensive. An $8\times8\times8$ mesh was used for $\mathrm{Im}\,\Sigma$.

[15] G.D. Mahan, *Many Particle Physics* (Plenum, New York, 1981), pp. 166–168.

[16] It has been demonstrated that in order to obtain good agreement between theory and experiment for the bandwidth of simple metals at $T=0$ using an LDA + GW approach, it is necessary to go beyond the random-phase approximation when determining the screened interaction. A Hubbard-type dielectric function based on LDA was used to calculate renormalized bandwidths in J.E. Northrop, M.S. Hybertsen, and S.G. Louie, Phys. Rev. B **59**, 819 (1987). We are mainly concerned with the general behavior of the bandwidth when the electron temperature is raised, so we use RPA in this work and leave a more accurate determination for later study.

[17] Note that the values for $\mathrm{Re}\,\Sigma$ in Fig. 6 are shifted slightly from those of Fig. 3. This is because we have included $v_{xc}(\mathbf{r})$ as it appears in Eq. (11) for the crystalline Al results. For jellium, $v_{xc}(\mathbf{r})$ is a constant, so we chose not to add it to $\mathrm{Re}\,\Sigma$. The addition of a constant to $\mathrm{Re}\,\Sigma$ does not change the relative quasiparticle energies (i.e., the bandwidth).

[18] G. Baym and L.P. Kadanoff, Phys. Rev. **124**, 287 (1961); F. Bechstedt, K. Tenelsen, B. Adolph, and R. DelSole, Phys. Rev. Lett. **78**, 1528 (1997).

[19] A recent approximate inclusion of vertex corrections in the self-consistent calculation of quasiparticle self-energies of the electon gas appears in Y. Takada, Phys. Rev. Lett. **87**, 226402 (2001).

[20] J.M. Ziman, *Models of Disorder* (Cambridge University Press, Cambridge, England, 1979), pp. 433–444.

[21] In addition, we have used the momentum operator (rather than the velocity operator) in the evaluation of dipole matrix elements. While this suffers from the neglect of the commutator of the nonlocal part of the pseudopotential with the position operator, this correction only changes the magnitude of $\epsilon_2^{inter}(\omega)$ by $\sim$10% and does not affect our general conclusions.

[22] N.W. Ashcroft and N.D. Mermin, *Solid State Physics* (W.B. Saunders Company, Philadelphia, 1976), p. 303.